의학석사 학위논문

Photoacoustic imaging for the differential diagnosis of cholesterol polyps from neoplastic polyps in the gallbladder

광음향영상을 이용한 담낭의 콜레스테롤 용종과 종양성 용종과의 감별에 관한 연구

2014 년 10 월

서울대학교 대학원

의학과 영상의학전공

채 희 동

Photoacoustic imaging for the differential diagnosis of cholesterol polyps from neoplastic polyps in the gallbladder

지도 교수 이 재 영

이 논문을 의학석사 학위논문으로 제출함
2014년 10월

서울대학교 대학원
의학과 영상의학 전공
채 희 동

채희동의 의학석사 학위논문을 인준함
2015년 1월

위 원 장 _____ (인)

부위원장 _____ (인)

위 원 _____ (인)

Abstract

Introduction: The differential diagnosis between cholesterol polyps and neoplastic polyps of gallbladder (GB) is important due to the malignant transformation potential of adenomas. Photoacoustic (PA) imaging is a new imaging technique with clinical potential in the real-time functional and molecular imaging. The purpose of our study was to assess the feasibility of ex vivo multispectral PA imaging in differentiating benign cholesterol polyps from adenomas and adenocarcinomas.

Methods: Surgically confirmed 24 polyps (17 cholesterol polyps, 4 adenomas, 3 adenocarcinomas) of 24 patients were prospectively included in this study between April 2014 and October 2014, with written informed consents. The surgical specimens were set on a scatter-free gel pad, which was immersed in a 0.9% saline-filled container. Then the PA intensities of polyps were measured for two separate wavelength intervals (421-647 nm, 692-917 nm). Mann-Whitney U test was performed for the comparison of normalized PA intensities between cholesterol and neoplastic polyps and between benign and malignant polyps. Then Kruskal-Wallis test was conducted for the comparison of normalized PA intensities among cholesterol polyps, adenomas, and adenocarcinomas.

Results: There were significant differences in the patient's age (P = .004) and size of the polyp (P = .015) among three groups. There was no significant difference in the normalized PA intensities between cholesterol polyps and

neoplastic polyps. But there were significant differences of the normalized PA intensities between benign and malignant polyps at 555 nm, 575 nm, 592 nm, 692 nm, 709 nm, 765 nm, 787 nm, 807 nm, 826 nm, and 853 nm ($P < 0.05$). The comparison of the normalized PA intensities among cholesterol polyps, adenomas, and adenocarcinomas demonstrated significant differences at 692 nm, 709 nm, 765 nm, 787 nm, and 853 nm ($P < 0.05$).

Conclusions: This preliminary result indicates that GB polyps might have different spectral pattern between benign and malignant polyps on multispectral PA imaging.

Keywords: Photoacoustic imaging, Gallbladder polyp, Cholesterol polyp, Gallbladder adenoma
Student Number: 2013-21704

CONTENTS

LIST OF TABLES AND FIGURES

LIST OF ABBREVIATION

PA = Photoacoustic

US = Ultrasonography

GB = Gallbladder

INTRODUCTION

The prevalence of gallbladder (GB) polyps is approximately 5 % in the adult population and these lesions are often detected incidentally by computed tomography (CT) scans or ultrasonography (US) imaging (1). Along with the increasing incidence of routine medical check-ups and recent technical improvements in diagnostic imaging, the detection of GB polyps is becoming more frequent (2). GB polyps can be classified as neoplastic polyps including adenomas and adenocarcinomas, or as nonneoplastic polyps including cholesterol polyps, inflammatory polyps and adenomyomatosis (3). Although most GB polyps are benign cholesterol polyps, current guidelines recommend surgical removal of GB polyps larger than 1 cm in view of the higher chance of malignancy (4, 5). But this approach not only imposes unnecessary anxiety on patients, but also carries with it significant socioeconomic burden to the community (5). Unfortunately none of the conventional imaging modalities including US, CT, magnetic resonance imaging, and endoscopic US (EUS) can accurately differentiate neoplastic and nonneoplastic polyps in the GB (2).

Photoacoustic (PA) imaging is a novel imaging technique with clinical potential in the real-time functional imaging. In PA imaging, a pulsed laser is illuminated to a biologic sample, then the light energy is deposited in the tissue leading to a transient temperature rise and thermoelastic expansion, which induce ultrasound waves (ie,

PA signals) (6, 7). Although they are very weak in intensity, the PA signals can be collected by using commercial US transducers (6). In contrast to conventional optical imaging, PA imaging is not limited by the light diffusion, but instead, is determined by the spatial resolution and tissue penetration of ultrasound (6, 8). Also contrary to the US in which the contrast depends on the acoustic impedance mismatch between different tissues, in the PA imaging, however, the tissue contrast is determined not by the mechanical and elastic properties of the tissue, but by its optical absorption, providing greater tissue differentiation and specificity than US (9). Along with this unique advantage of PA imaging, this technology has been applied to various medical fields, including the detection of the breast microcalcifications (10, 11), differentiation of benign and malignant lesions of thyroid glands (12, 13), and sentinel lymph node imaging (14). Since PA imaging is a real-time imaging modality with high spatial and contrast resolutions, it may also have an alternative role in the diagnosis of GB polyps.

Thus, the purpose of our study was to assess the feasibility of ex vivo multispectral PA imaging in differentiating benign cholesterol polyps from adenomas and adenocarcinomas.

MATERIALS AND METHODS

Study population

Our institutional review board approved this prospective study, and written informed consents were obtained from all patients. Twenty-four patients (mean age, 54.6 ± 14.7; range, 30-89 years) who underwent cholecystectomy from April 2014 to October 2014 constituted our study population. There were 9 men (mean age, 55.3 ± 18.4; range, 35-89 years) and 15 women (mean age, 54.2 ± 12.7; range, 30-74 years). All patients were clinically scheduled for surgery due to GB polyps detected on US or EUS. Among the 24 patients, 22 patients underwent laparoscopic cholecystectomy, one underwent open cholecystectomy, and one patient underwent extended cholecystectomy. Pathologically, resected polyps were confirmed as cholesterol polyps (n=17), adenomas (n=4), and adenocarcinomas (n=3).

Measurement of the photoacoustic signal

The experimental arrangement of the PA and US imaging data acquisition system was assembled similar to our previous experiments (10) (11). The specimens were fixed on a scatter-free gel pad (Aquaflex, Parker Lab, Inc., Farfield, NJ, US), which was then immersed in a 0.9% saline-filled container. The temperature of the container was maintained at 24℃. To obtain PA signals from the specimens,

radiofrequency echo data were acquired using a US transducer equipped with a SonixTouch research package (Ultrasonix Corp., Vancouver, BC, Canada) and a 7-MHz linear array (L14-5/38) connected to a SonixDAQ parallel system. The Q-switch trigger of a Nd:YAG laser excitation system (Surelite III-10 and Surelite OPO Plus, Continuum Inc., Santa Clara, CA, US) was then sent to a SonixTouch research package at the pulse repetition of 10 Hz. Laser was delivered by a custom bifurcated optic fiber bundle and optical fluency was focused at 30 mm depth from the array transducer (Fiberoptic Systems, Inc., Simi Valley, CA, US). Energy density of the laser was fixed around 19 mJ/cm^2 during the experiment to satisfy the regulation of ANSI Z136 radiation safety limit of 20 mJ/cm^2. By referring the Q-switch trigger, scanline data were stored in the dedicated acquisition system. The laser pulse length was 7 ns and its wavelength was controlled by a software program in a personal computer. The distance between the US transducer and specimen was 30 mm, which was longer than the transducer's elevational focal depth of 16 mm. The researchers performing all experimental procedures were blinded to the clinical information and pathologic results of specimens.

Data analysis

The measurement of the PA intensities of polyps was conducted for two separate wavelength intervals with 421-647 nm and 692-917 nm intervals. The PA spectrum acquired at each wavelength interval was normalized separately by dividing the PA intensity at each wavelength by the peak PA intensity in the interval. The

comparison of the mean normalized PA intensities was conducted between cholesterol polyps and neoplastic polyps (including adenomas and adenocarcinomas), between benign polyps (including cholesterol polyps and adenomas) and malignant polyps (adenocarcinomas), and among cholesterol polyps, adenomas, and adenocarcinomas. And the wavelengths showing the peak PA intensity and maximum intensity difference were also identified for each group.

To assess the differences in the patient's age, size of the polyp, and the mean normalized PA intensities among three groups, the Kruskal-Wallis test was used and was followed by the Dunn-Bonferroni test for pairwise comparisons. The Fisher's exact test and Mann-Whitney U test were performed respectively to compare the sex ratio and the mean normalized PA intensities between two groups (cholesterol vs neoplastic polyps and benign vs malignant polyps). Statistical analyses were performed using SPSS version 19.0 (SPSS Inc., Chicago, Ill, US). A *P*-value of <0.05 was considered to indicate a significant difference.

RESULTS

Study population characteristics

The sex distribution of patients did not show any significant differences between cholesterol and neoplastic polyps (P = .539) and between benign and malignant polyps (P = .308). There were significant differences in the patient's age (P = .004) and size of the polyp (P = .015) among three groups. The patients with cholesterol polyps were younger than those with adenocarcinomas (48.2 ± 10.8 versus 78.0 ± 9.6, P = .010). Also the mean size of cholesterol polyps was smaller than that of adenocarcinomas (0.9 ± 0.4 cm versus 2.6 ± 0.6 cm, P = .019). Table 1 summarizes the comparison of study population characteristics among cholesterol polyps, adenomas, and adenocarcinomas.

Table 1. ***Demographic data of patients***

Type	Sex (M/F)*	Age (y)†	Size (cm)‡
Cholesterol polyp (n=17)	6/11	48.2 ± 10.8	0.9 ± 0.4
Adenoma (n=4)	1/3	64.3 ± 8.4	1.5 ± 0.8
Adenocarcinoma (n=3)	2/1	78.0 ± 9.6	2.6 ± 0.6

Note—Data are mean ± standard deviation for age and size.
[*]*P* = .539 (cholesterol vs neoplastic polyp), .308 (benign vs malignant polyp), Fisher's exact test.
[†]*P* = .004, Kruskal-Wallis test (cholesterol polyp vs adenocarcinoma, *P* = .010; Dunn-Bonferroni test).
[‡]*P* = .015, Kruskal-Wallis test (cholesterol polyp vs adenocarcinoma, *P* = .019; Dunn-Bonferroni test).

Comparison of PA intensities of cholesterol polyps and neoplastic polyps

At shorter wavelengths between 421 and 647 nm, the normalized PA intensity of cholesterol polyps peaked at 459 nm with the mean value of 0.89. The peak intensity of neoplastic polyps was measured at 421 nm with the mean value of 0.81 (Fig 1(a)). At longer wavelengths interval between 692 and 917 nm, both the cholesterol polyps and neoplastic polyps showed the peak intensities at the wavelength of 692 nm with the mean normalized PA intensity of 0.97 in cholesterol polyps and 0.90 in neoplastic polyps (Fig 1(b)). The maximum difference was calculated to be 0.18 at the wavelength of 459 nm. But there was no significant difference of the normalized PA intensities at each wavelength between two groups.

(A)

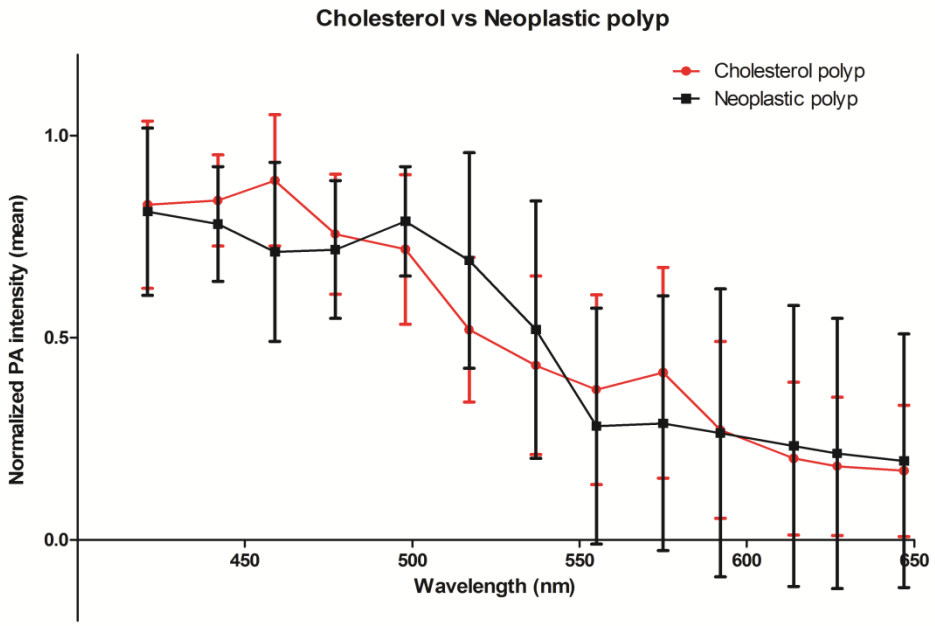
Cholesterol vs Neoplastic polyp
Cholesterol polyp
Neoplastic polyp
Normalized PA intensity (mean)
1.0
0.5
0.0
450
500
550
600
650
Wavelength (nm)

(B)

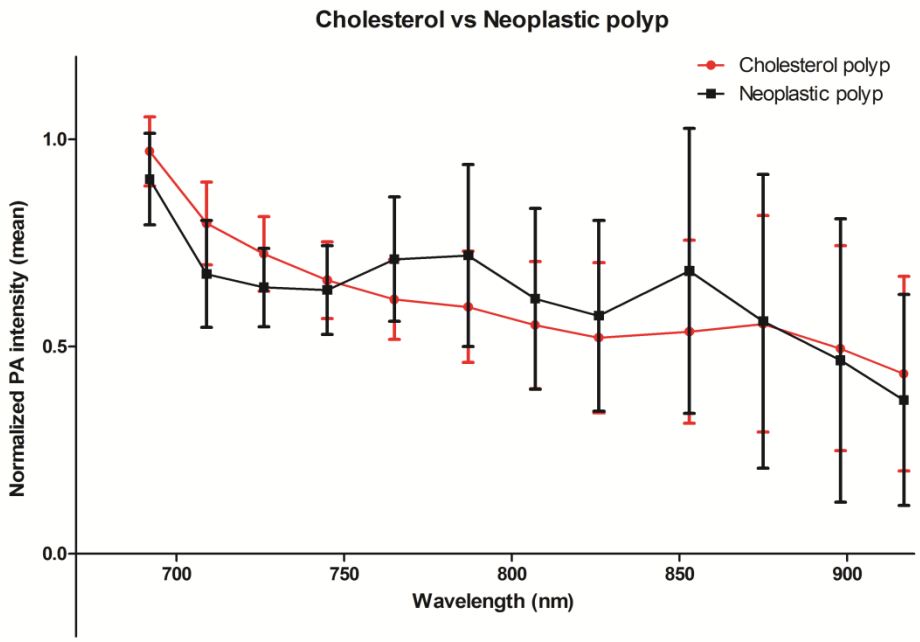

Figure 1. Normalized photoacoustic intensities of cholesterol and neoplastic polyps

The mean normalized photoacoustic intensities of cholesterol and neoplastic polyps (A) at the shorter wavelengths interval between 421 nm and 647 nm, (B) at the longer wavelengths interval between 692 nm and 917 nm. Error bars denote the standard deviation.

Comparison of PA intensities of benign polyps and malignant polyps

When the normalized PA intensities of benign polyps and malignant polyps were compared, the peak intensity of benign polyps was measured at 459 nm with the mean value of 0.86 at shorter wavelengths interval. The normalized PA intensity of malignant polyps peaked at 421 nm with the mean value of 0.91 (Fig 2(a)). At longer wavelengths interval, benign polyps showed the peak intensity at 692 nm with the mean normalized PA intensity of 0.97 and malignant polyps had the peak value of 0.97 at 853 nm (Fig 2(b)).

The Mann-Whitney U test revealed statistically significant differences of the normalized PA intensities between benign and malignant polyps at 555 nm (median, 0.34 vs 0.13; P = .041), 575 nm (median, 0.40 vs 0.04; P = .041), and 592 nm (median, 0.20 vs 0.05; P = .023) in shorter wavelengths interval and at 692 nm (median, 1.00 vs 0.91; P = .031), 709 nm (median, 0.81 vs 0.61; P = .011), 765 nm (median, 0.62 vs 0.79; P = .007), 787 nm (median, 0.55 vs 0.95; P = .007), 807 nm (median, 0.56 vs 0.76; P = .011), 826 nm (median, 0.52 vs 0.73; P = .031), and 853 nm (median, 0.47 vs 1.00; P = .002) in longer wavelengths interval. The maximum difference was obtained at 853 nm with the mean values of 0.52 and 0.97, respectively (Fig 2).

(A)

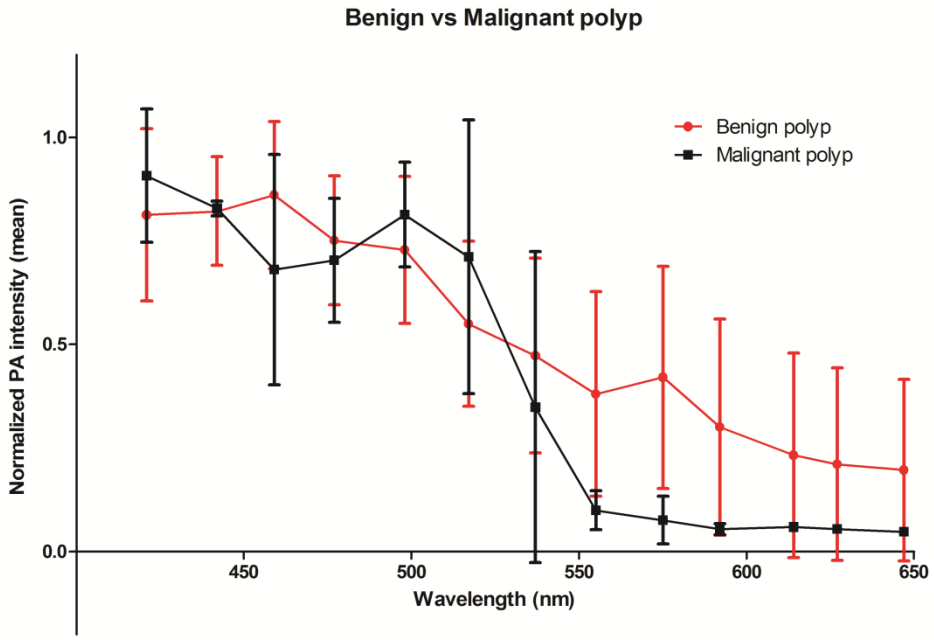
Benign vs Malignant polyp
Benign polyp
Malignant polyp
Normalized PA intensity (mean)
1.0
0.5
0.0
450
500
550
600
650
Wavelength (nm)

(B)

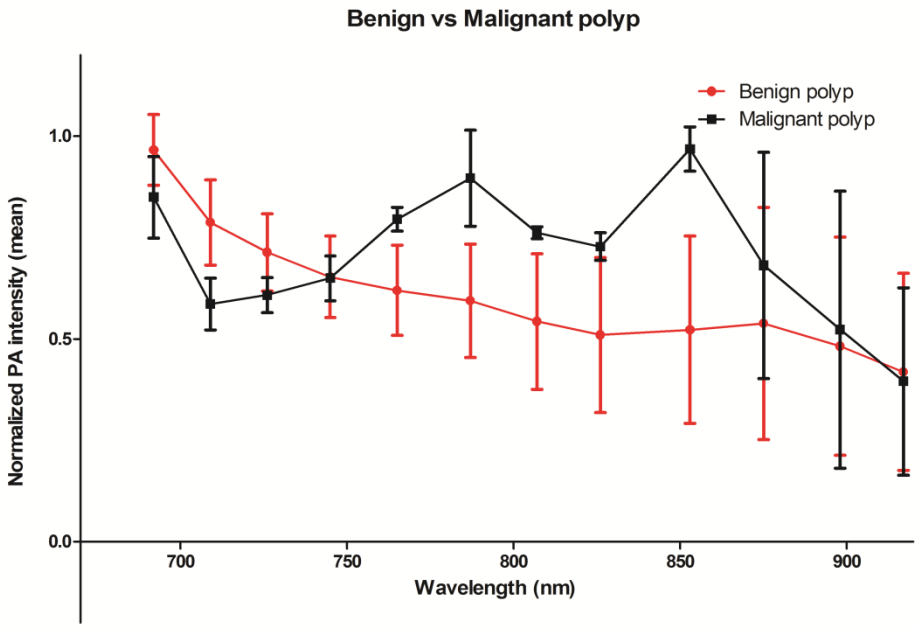

Figure 2. Normalized photoacoustic intensities of benign and malignant polyps

The mean normalized photoacoustic intensities of benign and malignant polyps (A) at the shorter wavelengths interval between 421 nm and 647 nm, (B) at the longer wavelengths interval between 692 nm and 917 nm. Error bars denote the standard deviation. Malignant polyps had significantly lower photoacoustic intensities at the wavelengths of 555-592 nm and 692-709 nm, and showed higher photoacoustic intensities at the wavelengths of 765-853 nm than benign polyps.

Comparison of PA intensities of cholesterol polyps, adenomas, and adenocarcinomas

The comparison of the normalized PA intensities among cholesterol polyps, adenomas, and adenocarcinomas with the Kruskal-Wallis test demonstrated that there were significant differences at the wavelengths of 692 nm (P = .017), 709 nm (P = .050), 765 nm (P = .040), 787 nm (P = .045), and 853 nm (P = .027). And the results of post hoc test using the Dunn-Bonferroni method showed that the normalized PA intensities of adenocarcinomas were significantly lower than those of cholesterol polyps at the wavelengths of 692 nm (median, 1.00 vs 0.91; P = .013) and 709 nm (median, 0.81 vs 0.61; P = .043). In contrast, adenocarcinomas had significantly higher intensities than cholesterol polyps at the wavelengths of 765 nm (median, 0.61 vs 0.79; P = .034), 787 nm (median, 0.55 vs 0.95; P = .045), and 853 nm (median, 0.47 vs 1.00; P = .032) (Fig 3). Representative cases are shown in Figure 4.

(A)

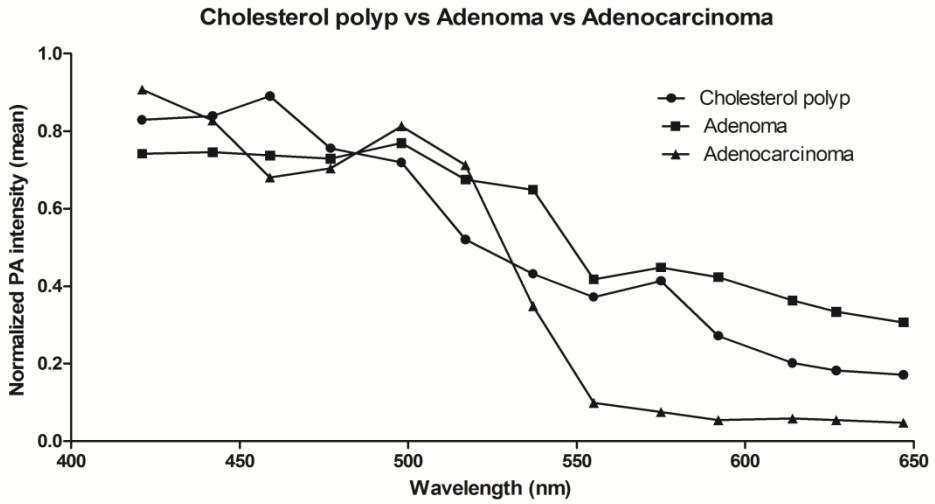

(B)

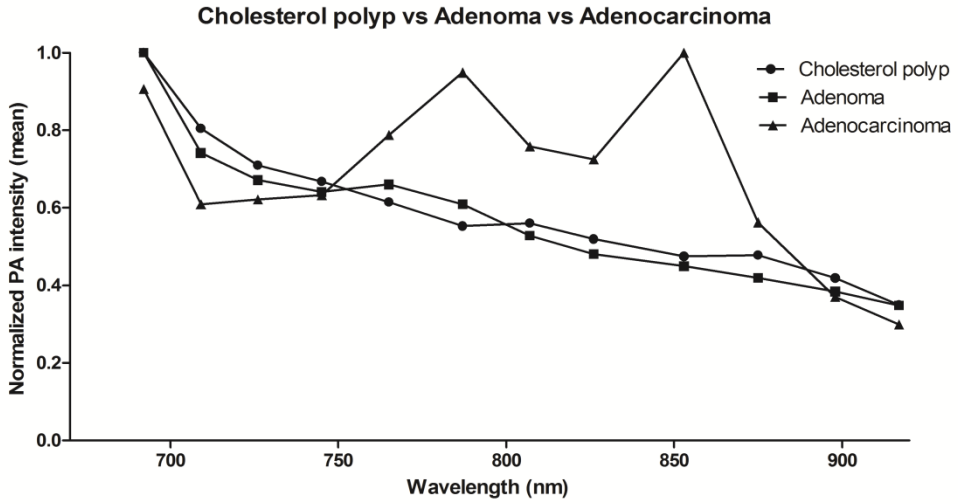

Figure 3. Normalized photoacoustic intensities of cholesterol polyps, adenomas, and adenocarcinomas

The mean normalized photoacoustic intensities of cholesterol polyps, adenomas,

and adenocarcinomas (A) at the shorter wavelengths interval between 421 nm and 647 nm, (B) at the longer wavelengths interval between 692 nm and 917 nm. Normalized photoacoustic intensities of adenocarcinomas were significantly lower than those of cholesterol polyps at 692 nm, 709 nm and were significantly higher at 765 nm, 787 nm, and 853 nm.

(A)

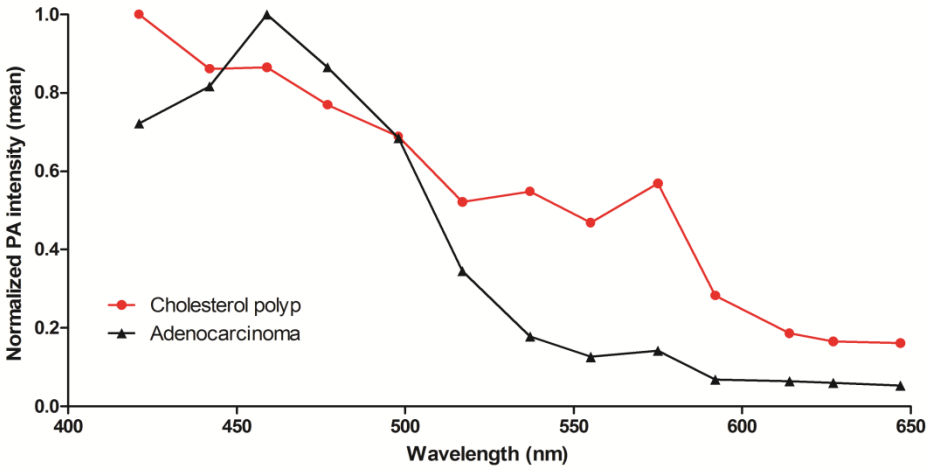

(B)

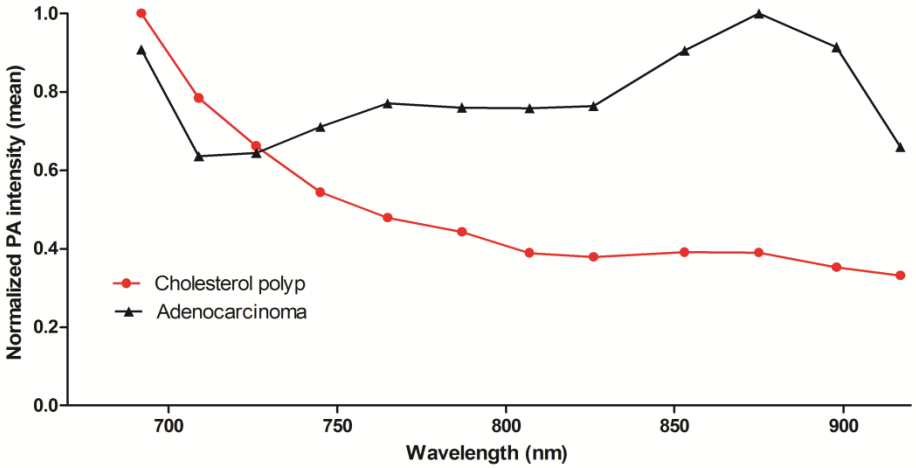

Figure 4. Normalized photoacoustic intensities of a cholesterol polyp and an adenocarcinoma

The mean normalized photoacoustic intensities of the cholesterol polyp in a 35-year-old woman and the adenocarcinoma in a 89-year-old man (A) at the shorter

wavelengths interval between 421 nm and 647 nm, (B) at the longer wavelengths interval between 692 nm and 917 nm. Two polyps show distinct photoacoustic spectral patterns: the photoacoustic intensity of the cholesterol polyp continuously decreases at 692-917 nm, while the adenocarcinoma presents absorption peak at 875 nm.

DISCUSSION

The differential diagnosis between nonneoplastic polyps and neoplastic polyps is important in the clinical management of the patients with GB polyps. The majority of GB polyps are nonneoplastic lesions such as cholesterol polyps and these lesions do not need to be resected (1). Rarely, however, these lesions may be neoplastic, and the primary concern is that they can be transformed into malignant lesions (4). And because of the extremely poor prognosis of GB cancer, it is also essential to accurately differentiate between benign and malignant polyps (15). According to current guidelines depending on size criteria, surgical removal is recommended for polyps greater than 10 mm and US follow-up for polyps smaller than 10 mm (4, 16). Consequently, cholesterol polyps larger than 10 mm and neoplastic polyps smaller than 10 mm could be misdiagnosed (1).

Advances in diagnostic imaging have steadily increased the sensitivity for the detection of GB polyps. But until now, there have been no available imaging modalities that can reliably distinguish polypoid lesions of GB or can predict the presence of malignancy. US is the most commonly used method for the diagnosis of GB polyps (17), but US is unable to accurately differentiate neoplastic polyps from nonneoplastic polyps because of their similar echogenicity and morphology (18-20). Other imaging modalities such as CT also have been used to examine GB polyps, but CT has the limitation in clearly depicting the shape and internal features of small lesions, and the differential diagnosis remains difficult in many cases (21-23)

There were several studies based on novel US techniques to overcome the shortcomings of conventional US imaging. Teber et al. (24) have evaluated the feasibility of real-time US elastography in GB polyps, and found that benign GB polyps had a high-strain elastographic pattern. In the studies using real-time contrast-enhanced (CE) EUS, GB adenomas showed homogeneous enhancement pattern in contrast to cholesterol polyps showing heterogeneous enhancement pattern (1). And malignant lesions showed rapid washout features after contrast agent administration on CE US (25).

To our knowledge, this is the first study that utilized PA imaging in the evaluation of the GB polyps. In the present study, benign and malignant polyps showed different photoacoustic characteristics. Malignant polyps had significantly lower PA intensities at the wavelengths of 555-592 nm and 692-709 nm, and showed higher PA intensities at the wavelengths of 765-853 nm than benign polyps. The maximum intensity difference between two groups was obtained at 853 nm. According to the known absorption spectra of biologic tissues, the wavelengths of 760 nm and 850 nm represent deoxyhemoglobin (Hb) and oxyhemoglobin (HbO_2), respectively (13, 26). From the results, it is possible that the higher tissue Hb and HbO_2 levels in the malignant lesion may have affected the optical absorption properties of tissue at this interval.

Cholesterol polyps result from abnormal deposits of triglycerides, cholesterol precursors, and cholesterol esters in macrophages in the gallbladder wall (27). In contrast, GB adenomas and adenocarcinomas are epithelial tumors composed of

cells resembling biliary epithelium. We hypothesized that these histopathological differences of two lesions would result in different PA spectral patterns. But in this study, there were no significant differences in the normalized PA intensities between two groups. Because of the abundance of C-H bonds and low water content compared with other soft tissues, lipid absorbs strongly at the near infrared wavelength range (around 1720 nm) (28, 29). Further investigation at this infrared spectral region would be needed to precisely reflect the optical absorption of lipid-rich tissues.

Our study has several limitations. First, our sample size is relatively small as it is one of the preliminary studies about PA imaging of GB polyps. Therefore, further studies with larger sample size will be necessary. Second, since this is an ex vivo study with surgical specimens, practical application might still be limited especially due to relatively thick abdominal wall that PA wave should pass through. But, PA imaging has a major advantage over existing optical modalities in optically scattering tissue even when the imaging depth is beyond the optical mean free path (6). As an example, PA imaging of the human breast has been achieved recently with satisfactory spatial resolution at a depth of up to 5 cm from the skin surface (30). Further studies with a sophisticated PA transducer using endoscopic probe might further facilitate its in-vivo use.

In conclusion, malignant and benign polyps of GB show distinguishable PA spectral pattern. The preliminary results of this ex vivo study indicate that multispectral PA imaging can be used in the differentiation of malignant and benign

GB polyps.

REFERENCES

1. Park CH, Chung MJ, Oh TG, Park JY, Bang S, Park SW et al. Differential diagnosis between gallbladder adenomas and cholesterol polyps on contrast-enhanced harmonic endoscopic ultrasonography. Surgical endoscopy 2013;27:1414-1421
2. Kwon W, Jang JY, Lee SE, Hwang DW, Kim SW. Clinicopathologic features of polypoid lesions of the gallbladder and risk factors of gallbladder cancer. Journal of Korean medical science 2009;24:481-487
3. Christensen AH, Ishak KG. Benign tumors and pseudotumors of the gallbladder. Report of 180 cases. Archives of pathology 1970;90:423-432
4. Corwin MT, Siewert B, Sheiman RG, Kane RA. Incidentally detected gallbladder polyps: Is follow-up necessary?--long-term clinical and us analysis of 346 patients. Radiology 2011;258:277-282
5. Lee KF, Wong J, Li JC, Lai PB. Polypoid lesions of the gallbladder. American journal of surgery 2004;188:186-190
6. Xu G, Meng ZX, Lin JD, Yuan J, Carson PL, Joshi B et al. The functional pitch of an organ: Quantification of tissue texture with

photoacoustic spectrum analysis. Radiology 2014;271:248-254

7. Kruger RA. Photoacoustic ultrasound. Med Phys 1994;21:127-131

8. Rich LJ, Seshadri M. Photoacoustic imaging of vascular hemodynamics: Validation with blood oxygenation level-dependent mr imaging. Radiology 2014:140654

9. Beard P. Biomedical photoacoustic imaging. Interface Focus 2011;1:602-631

10. Kim GR, Kang J, Kwak JY, Chang JH, Kim SI, Youk JH et al. Photoacoustic imaging of breast microcalcifications: A preliminary study with 8-gauge core-biopsied breast specimens. PloS one 2014;9:e105878

11. Kang J, Kim EK, Kim GR, Yoon C, Song TK, Chang JH. Photoacoustic imaging of breast microcalcifications: A validation study with 3-dimensional ex vivo data and spectrophotometric measurement. Journal of biophotonics 2013

12. Kang J, Chung WY, Kang SW, Kwon HJ, Yoo J, Kim EK et al. Ex vivo estimation of photoacoustic imaging for detecting thyroid microcalcifications. PloS one 2014;9:e113358

13. Dogra VS, Chinni BK, Valluru KS, Moalem J, Giampoli EJ, Evans K et al. Preliminary results of ex vivo multispectral photoacoustic

imaging in the management of thyroid cancer. AJR. American journal of roentgenology 2014;202:W552-558

14. Erpelding TN, Kim C, Pramanik M, Jankovic L, Maslov K, Guo Z et al. Sentinel lymph nodes in the rat: Noninvasive photoacoustic and us imaging with a clinical us system. Radiology 2010;256:102-110

15. Song ER, Chung WS, Jang HY, Yoon M, Cha EJ. Ct differentiation of 1-2-cm gallbladder polyps: Benign vs malignant. Abdominal imaging 2014;39:334-341

16. Pedersen MR, Dam C, Rafaelsen SR. Ultrasound follow-up for gallbladder polyps less than 6 mm may not be necessary. Danish medical journal 2012;59:A4503

17. Jang JY, Kim SW, Lee SE, Hwang DW, Kim EJ, Lee JY et al. Differential diagnostic and staging accuracies of high resolution ultrasonography, endoscopic ultrasonography, and multidetector computed tomography for gallbladder polypoid lesions and gallbladder cancer. Annals of surgery 2009;250:943-949

18. Andren-Sandberg A. Diagnosis and management of gallbladder polyps. North American journal of medical sciences 2012;4:203-211

19. Zielinski MD, Atwell TD, Davis PW, Kendrick ML, Que FG. Comparison of surgically resected polypoid lesions of the gallbladder

to their pre-operative ultrasound characteristics. Journal of gastrointestinal surgery : official journal of the Society for Surgery of the Alimentary Tract 2009;13:19-25

20. Damore LJ, 2nd, Cook CH, Fernandez KL, Cunningham J, Ellison EC, Melvin WS. Ultrasonography incorrectly diagnoses gallbladder polyps. Surgical laparoscopy, endoscopy & percutaneous techniques 2001;11:88-91

21. Park KW, Kim SH, Choi SH, Lee WJ. Differentiation of nonneoplastic and neoplastic gallbladder polyps 1 cm or bigger with multi-detector row computed tomography. Journal of computer assisted tomography 2010;34:135-139

22. Azuma T, Yoshikawa T, Araida T, Takasaki K. Differential diagnosis of polypoid lesions of the gallbladder by endoscopic ultrasonography. American journal of surgery 2001;181:65-70

23. Furukawa H, Takayasu K, Mukai K, Inoue K, Kyokane T, Shimada K et al. Ct evaluation of small polypoid lesions of the gallbladder. Hepato-gastroenterology 1995;42:800-810

24. Teber MA, Tan S, Donmez U, Ipek A, Ucar AE, Yildirim H et al. The use of real-time elastography in the assessment of gallbladder polyps: Preliminary observations. Medical ultrasonography

2014;16:304-308

25. Xie XH, Xu HX, Xie XY, Lu MD, Kuang M, Xu ZF et al. Differential diagnosis between benign and malignant gallbladder diseases with real-time contrast-enhanced ultrasound. European radiology 2010;20:239-248

26. Vogel A, Venugopalan V. Mechanisms of pulsed laser ablation of biological tissues. Chemical reviews 2003;103:577-644

27. Berk RN, van der Vegt JH, Lichtenstein JE. The hyperplastic cholecystoses: Cholesterolosis and adenomyomatosis. Radiology 1983;146:593-601

28. Wang B, Karpiouk A, Yeager D, Amirian J, Litovsky S, Smalling R et al. In vivo intravascular ultrasound-guided photoacoustic imaging of lipid in plaques using an animal model of atherosclerosis. Ultrasound in medicine & biology 2012;38:2098-2103

29. Anderson RR, Farinelli W, Laubach H, Manstein D, Yaroslavsky AN, Gubeli J, 3rd et al. Selective photothermolysis of lipid-rich tissues: A free electron laser study. Lasers in surgery and medicine 2006;38:913-919

30. Xie Z, Hooi FM, Fowlkes JB, Pinsky RW, Wang X, Carson PL. Combined photoacoustic and acoustic imaging of human breast

specimens in the mammographic geometry. Ultrasound in medicine & biology 2013;39:2176-2184

국문 초록

서론: 담낭 선종은 악성 전환의 위험이 있기 때문에 적절한 치료를 위하여 담낭의 콜레스테롤 용종과 선종을 감별하는 것은 중요하다. 광음향영상은 최근 임상적으로 실시간 기능 영상 및 분자 영상이 가능한 새로운 영상 기법으로 각광받고 있다. 본 연구에서는 광음향 영상을 이용하여 콜레스테롤 폴립과 담낭 선종 및 담낭 선암의 감별을 위한 실험적 연구를 시행하였다.

방법: 2014 년 4 월부터 2014 년 10 월까지, 24 명의 담낭 용종을 갖는 환자를 모집하였다. 환자의 동의 하에 담낭 절제술로부터 적출한 담낭 용종을 젤 패드에 고정 후 식염수에 침전시키고 이후 421-647 nm 와 692-917 nm 의 두 구간의 파장대의 레이저를 이용하여 용종 절편 및 인접한 정상 담낭 벽 조직에 대해 광음향 신호를 측정하였다. 콜레스테롤 용종군과 종양성 용종군 및 양성 용종군과 악성 용종군의 정규화된 광음향 신호의 차이를 비교하기 위하여 Mann-Whitney U 검정을 시행하였다. 이후 콜레스테롤 용종군 및 담낭 선종군과 담낭 선암군 간의 정규화된 광음향 신호의 차이를 비교하기 위하여 Kruskal-Wallis 검정을 시행하였다.

결과: 콜레스테롤 용종군과 담낭 선종군은 환자 연령 (P = .004) 및 용종 크기 (P = .015)에서 유의한 차이를 보였다. 각각의 파장대에서 조사한 정규화 광음향 신호는 콜레스테롤 용종군과 종양성 용종군을 비교하였을 때에는 유의한 차이를 보이지 않았다. 그러나, 양성 용종군과 악성 용종군을 비교하였을 때에는 555 nm 및 575 nm, 592 nm, 692 nm, 709 nm, 765 nm, 787 nm, 807 nm, 826 nm, 853 nm 파장대에서 정규화 광음향 신호에 유의하게 차이가 있었다 (P < 0.05). 콜레스테롤 용종군 및 담낭 선종군, 담낭 선암군의 세 군을 비교하였을 때에는 692 nm 및 709 nm, 765 nm, 787 nm, 853 nm 파장대에서 정규화 광음향 신호의 유의한 차이가 있었다 (P < 0.05)

결론: 담낭의 양성 용종 및 악성 용종은 고유의 광음향 신호 스펙트럼을 가질 것으로 예측되며, 광음향 영상을 이용하여 두 질환군의 감별진단에 도움이 될 수 있다.

주요어 : 광음향 영상, 담낭 용종, 콜레스테롤 용종, 담낭 선종

학 번 : 2013-21704